Rapid Communication

Orbital responses to methyl sites in C_nH_{2n+2} ($n = 1$–6)*

Yang Ze-Jin(杨则金)[a)†], Cheng Xin-Lu(程新路)[b)],
Zhu Zheng-He(朱正和)[b)], and Yang Xiang-Dong(杨向东)[b)]

[a)] *School of Science, Zhejiang University of Technology, Hangzhou* 310023, *China*
[b)] *Institute of Atomic and Molecular Physics, Sichuan University, Chengdu* 610065, *China*

(Received 4 September 2011; revised manuscript received 13 October 2011)

Orbital responses to methyl sites in C_nH_{2n+2} ($n = 1$–6) are studied by B3LYP/TZVP based on the most stable geometries using the B3LYP/aug-cc-pVTZ method. Vertical ionization energies are produced using the SAOP/et-pVQZ model for the complete valence space. The highest occupied molecular orbital (HOMO) investigations indicate the p-electron profiles in methane, ethane, propane, and n-butane. By increasing the number of carbon–carbon bonds in lower momentum regions, the s, p-hybridized orbitals are built and display strong exchange and correlation interactions in lower momentum space ($P \lesssim 0.50$ a.u.). Meanwhile, the relative intensities of the isomers in lower momentum space show the strong bonding number dependence of the carbon–carbon bonds, meaning that more electrons have contributed to orbital construction. The study of representative valence orbital momentum distribution further confirms that the structural changes lead to evident electronic rearrangement over the whole valence space. An analysis based on the isomers reveals that the valence orbitals are isomer-dependent and the valence ionization energy experiences an apparent shift in the inner valence space. However, such shifts are greatly reduced in the outer valence space. Meanwhile, the opposite energy shift trend is found in the intermediate valence space.

Keywords: electron momentum spectroscopy, valence ionization energy, charge density distribution

PACS: 34.50.–S, 34.50.Gb, 34.80.–I, 34.80.Gs **DOI:** 10.1088/1674-1056/21/2/023401

1. Introduction

Electron momentum spectroscopy (EMS), which is used to simultaneously measure valence binding energies and electron momentum distributions, is a powerful technique to investigate the electronic structures of atoms and molecules. EMS as an experimental method and the theoretical interpretations of its measured results for atoms and molecules have been developed over the last four decades and EMS is shown to have great potential for exploring atomic and molecular structures.[1−31]

Small saturated hydrocarbons C_nH_{2n+2} ($n = 1$–6) have been investigated extensively both theoretically and experimentally by EMS.[19,22,32−51] Previous studies have focused mainly on frontier orbitals for individual species and thus little information can be obtained about the inner valence orbitals till now. It is worthwhile to systematically study several small saturated hydrocarbons to explore the relationships of the valence orbital variations with their corresponding structural rearrangements. EMS is a unique technique by means of which additional information about orbital and chemical bonding for such isomers can be obtained in momentum space.

To the best of the authors' knowledge, no detailed study has been reported for the small saturated alkanes C_nH_{2n+2} ($n = 1$–6). Therefore, in this paper, we will concentrate on information concerning the momentum distributions of valence orbitals and their isomer dependence. At the same time, the valence vertical ionization energies of the species caused by their chemical shift will be compared.

2. Methods and computational details

The density functional theory (DFT) based hybrid B3LYP (embedded in Gaussian 03) functional with Dunning's augmented correlation corrected triple zeta plus polarization Gaussian basis set,

*Projects supported by the National Natural Science Foundation of China (Grant Nos. 10974139, 11104247, and 11176020).
†Corresponding author. E-mail: zejinyang@yahoo.com.cn
© 2012 Chinese Physical Society and IOP Publishing Ltd

i.e., B3LYP/aug-cc-pVTZ, was used to optimize the ground state geometries for C_nH_{2n+2} (n = 1–6), and the wavefunctions in coordinate space were calculated by B3LYP/TZVP (the TZVP is a triple zeta valence polarized Gaussian basis set) based on the most stable geometries. Orbital ionization energies of the whole valence space were simulated using the selected SAOP/et-pVQZ models[52] embedded in ADF 2008 code.[53] The selected SAOP model has been proven to be an effective way to describe ionization potentials (IPs) in the entire valence shell.[37] Molecular orbitals (MOs) obtained in coordinate space (based on the B3LYP/TZVP model) were directly mapped into momentum space as theoretical momentum distributions (TMDs). The Fourier transform and a number of approximations such as the Born–Oppenheimer approximation, the independent particle approximation, and the plane wave impulse approximation (PWIA),[54] were employed.

Within these approximations, the EMS cross-section for randomly oriented gas-phase molecules with unresolved rotational and vibrational states is given by[55]

$$\sigma_{\mathrm{EMS}} \propto \int \mathrm{d}\Omega \left| \left\langle p\Psi_{\mathrm{f}}^{N-1} \middle| \Psi_{\mathrm{i}}^{N} \right\rangle \right|^2, \qquad (1)$$

where $\int \mathrm{d}\Omega$ denotes spherical averaging over the full solid angle to account for the random orientation of the gaseous target molecules; p is a plane-wave spin–orbital momentum for an electron at the instant of ionization; Ψ_{f}^{N-1} and Ψ_{i}^{N} are the total electronic wavefunctions of the final ion state and the target molecule ground (initial) state, respectively. The overlap of the N-electron initial neutral state wavefunctions and (N–1)-electron final ion state wavefunctions of a target in Eq. (1) is known as the Dyson orbital. The Dyson orbital may be regarded as a "dynamic" type of orbital in that it is describing the process of electron transfer, i.e., how an electron "is ejected from" a molecular orbital in a molecule, a concept that is eminently useful for understanding chemical reactivity and bonding.

The Dyson orbital for electron transfer (i.e., ionization) can be very closely approximated by the initial state Kohn–Sham (KS) orbital of DFT,[56] which is known as the target KS approximation. With these further approximations the relative (e, 2e) cross section becomes

$$\sigma_{\mathrm{EMS}} \propto \int \mathrm{d}\Omega \left| \varphi_j^{\mathrm{KS}}(p) \right|^2, \qquad (2)$$

where $\varphi_j^{\mathrm{KS}}(p)$ is the one-electron momentum space canonical (i.e., delocalized) KS orbital wavefunction for the j-th electron, corresponding to the orbital from which the electron is ionized. It should be noted that accounting for electron correlation effects in the target ground state is included in the KS approximation via the exchange correlation potential, and the detailed descriptions can be found elsewhere.[56] Note also that the momentum space representation $\varphi_j^{\mathrm{KS}}(p)$ is the Fourier transform (by a modified HEMS code[54]) of the position space one-electron wave function $\varphi_j^{\mathrm{KS}}(r)$.

3. Results and discussion

3.1. Isomer dependence of the HOMOs

We employ the B3LYP/TZVP//B3LYP/aug-cc-pVTZ method which has also been used in previous studies[49,50] for simulating orbital momentum distributions and geometry optimizations, and the simulation results are in excellent agreement with experimental data, which confirms that DFT can produce reliable results despite the dynamic instabilities in lower momentum space.[32] Detailed comparisons between experimental data and theoretical calculations for methane,[33,34,36] ethane,[35,39] propane,[38,41–43] n-butane,[37,45,47,49,51] and isobutane[40,44,48] can be found elsewhere, and the good agreement confirms that DFT is the best choice. Here, we only give the systematic trends of the orbital momentum distributions for C_nH_{2n+2} (n = 1–6) to obtain a more general conclusion.

Figures 1–4 show the simulated HOMOs of C_nH_{2n+2} (n = 1–6). Figure 1 shows the HOMOs of methane, ethane, and propane in dual space, i.e., coordinate and momentum space. From Fig. 1 we can see that the p-electron dominated profiles have been built in momentum space, and their relative intensities show certain symmetry dependences, such as their relative intensities in descending order, i.e., $1t_2 > 1e_{\mathrm{g}} > 2b_1$, which is consistent with the cases of their different degrees of degeneracy and symmetries. From further analysis of ethane and propane it is easily found that π bonds are formed by p_z electrons.

Figure 2 shows the s, p-hybridized and p-dominated HOMOs of isobutane and n-butane, respectively. As shown in Fig. 2, the isomerization has changed the relative intensities of the profiles particularly for lower momentum components. According to Fig. 2 it is clearly seen that isobutane presents an s-dominated ($P \lesssim 0.5$ a.u.) and a significant p-contributed ($\sim$ 0.5–1.5 a.u.) profile, indicating an s, p-mixed orbital. However, n-butane has presented a

p-dominated HOMO, consistent with the profiles of methane, ethane, and propane, indicating that they have the same bonding mechanism and electron density distributions. Moreover, comparison of charge density distribution between isobutane and n-butane from coordinate space demonstrates that the δ bond of n-butane has been converted into a π bond of isobutane.

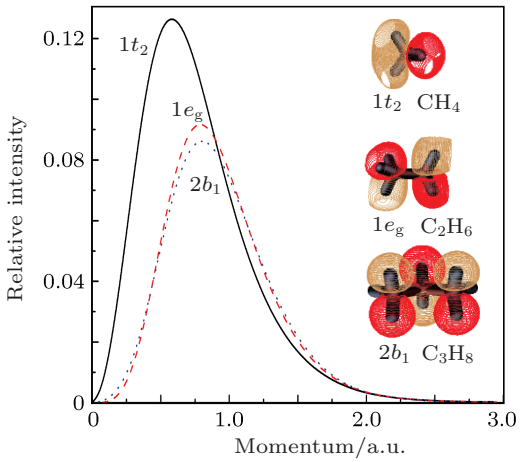


Fig. 1. (colour online) HOMOs of methane, ethane, and propane.

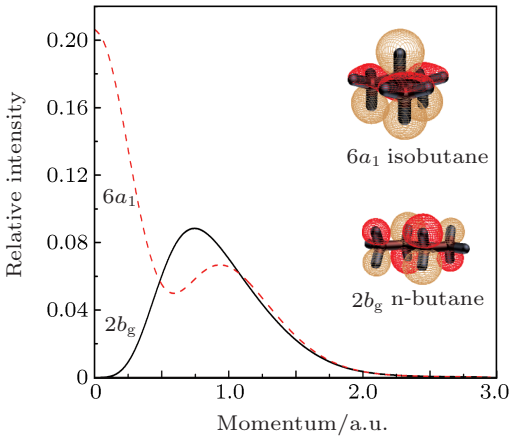


Fig. 2. (colour online) HOMOs of n-butane and isobutene.

Figure 3 shows the HOMOs of n-pentane, isopentane, and neopentane. To date and to the authors' knowledge, no experimental measurements have been performed for pentane and hexane and the present theoretical investigations thus could provide a systematical insight into understanding the structural-dependent orbital responses. Figure 3 reveals the complicated orbital shapes and strong responses particularly in lower momentum space, whereas the variations decrease gradually with momentum and their differences produced in higher momentum regions can also be completely neglected. The unique nonzero relative intensity of isopentane at zero momentum indicates that partial s electrons have contributed to chemical bonding and reflect their s, p-mixed hybridization orbital nature, differing from the other two p-dominated orbitals. From further analysis it follows that the relative intensities have shown a strong bonding number dependence of the carbon–carbon bonds in lower sensitive regions, such as the relative intensities in descending order for neopentane, isopentane, and n-pentane, i.e., $4t_2 > 21a > 7b_2$, which just corresponds to the sequence of their numbers of the carbon atoms bonded with the other surrounding carbon atoms. The above conclusions can also be confirmed by the electron charge density distributions in coordinate space, such as neopentane that has more significant electron interactions than the other two isomers. Moreover, the three isomers display more p_x and p_y electron contributions than p_z.

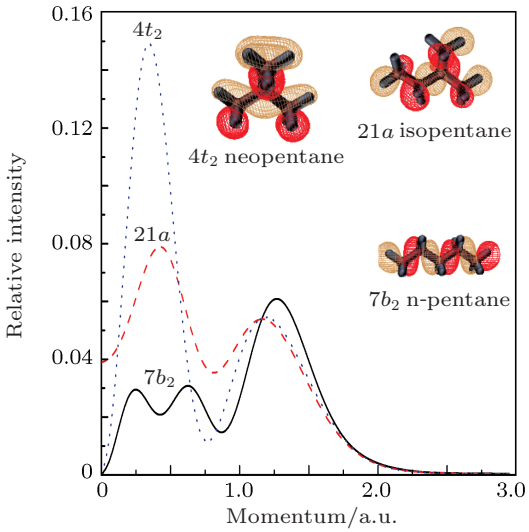


Fig. 3. (colour online) HOMOs of n-pentane, isopentane, and neopentane.

In Fig. 4, the five HOMOs of hexane show similar trends in orbital profiles and relative intensity variations to those of pentanes, i.e., significant intensity changes occur in lower momentum regions and their differences decrease gradually with increasing momentum. The relative intensities in lower momentum regions are in descending order, i.e., $17a' > 13a_g > 25a \approx 10a'' > 10a_g$, which once again demonstrates that the more the carbon atoms bonded with the other surrounding carbon atoms, the higher the relative intensity could be. Similar to the cases of the three isomers of pentane, the five isomers of hexane each also show two small peaks in lower momentum regions and the two small peaks overlap into one strong peak with the increase of the degree of branching in the

backbone. The near-zero value of the relative intensity at zero momentum of 2, 3-dimethylbutane and 2, 2-dimethylbutane further demonstrates that few s electrons are involved in chemical bonding during isomerization. Therefore, all the five isomers present p-dominated orbital momentum distributions, differing from the cases of pentane and butane. Meanwhile, they are well matched by the electron charge density distributions in coordinate space and present similar variations to those in the cases of pentane.

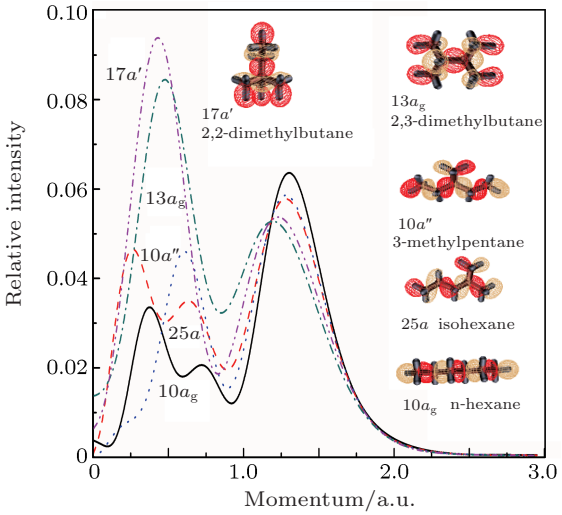


Fig. 4. (colour online) HOMOs of n-hexane and its four isomers.

3.2. Isomer dependence of the internal MOs

Deep analysis of the internal MOs can reveal more comprehensive bonding and orbital variation information related to the shift of the methyl functional group. Studies of valence orbital energy are essential and capable of revealing individual orbital distribution information, through which the orbital energy level shift relative to those of its isomers can also be obtained and thus could provide a deeper understanding of macroscopic properties. For the sake of completeness, we also study all the orbital momentum distributions and select some representative ones to clarify their structure-based responses and dependences caused by one methyl shift. Here, we select orbitals with ionization potentials (IPs) being 0.5 eV larger than that of n-alkanes (with the exception of MO10). The IPs for the whole valence space are calculated by the SAOP/et-pVQZ method. Note that SAOP can generate vertical ionization potential energies of molecular species with an accuracy of up to 0.2 eV using the "meta-Koopmans" theorem[57–59] as Koopmans' theorem does not hold for KS orbital energies, and is particularly successful in modeling the exchange correlation functional.[60]

In Figs. 5(a) and 5(b), the valence energy shifts of isobutane with respect to n-butane are presented, together with their dual space electron charge density distributions. From Fig. 5 we can see that MO6, MO7, and MO12 (we have defined the innermost core orbital as MO1) have great changes compared with other valence orbitals, in particular MO7 (the momentum and electron charge density distributions are briefly introduced without IP explanations in Ref. [22]) presents the largest energy shift (1.25 eV), which is consistent with the cases of their orbital momentum distributions and electron charge density distributions. The energy level shifts of the other 13 (including MO10) valence orbitals are smaller than 0.5 eV, particularly for the HOMO, it has negligible variations. Therefore, the methyl shift has caused significant changes for most of the orbitals, particularly for the inner ones.

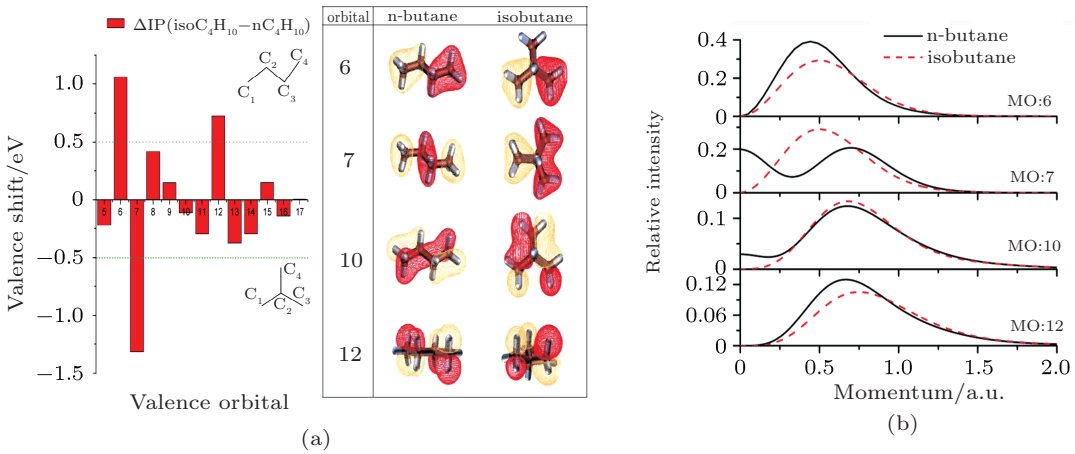


Fig. 5. (colour online) Valence energy shift of n, iso-C_4H_{10} (a) and relative intensities (b) of n, iso-C_4H_{10}.

In Figs. 6(a) and 6(b), neopentane presents a more significant variation than isopentane during isomerizations particularly in the inner valence space. From the analyses of all the valence orbitals we find that MO9 presents the most significant shifts: 2.13 eV in neopentane, 0.65 eV in isopentane, and the second one MO7 presents the shifts: 1.75 eV in neopentane and 0.5 eV in isopentane. From the calculations it follows that there are five orbitals whose shifts are larger than 0.5 eV in neopentane, reflecting the strong layout dependence of the orbitals as there are only two orbitals with the same variations in isopentane. Moreover, these changes appear mainly in the inner valence regions. Also, we find that the second HOMOs of isopentane and neopentane have experienced small significant variations compared with that of n-pentane. Further studies of these selected valence orbitals about their momentum distributions confirm once again that the corresponding orbital intensities and shapes display great changes, indicating that the different valence-shell electrons contribute to the orbital bonding. Furthermore, we also find that the orbital energy shifts of isopentane and neopentane present similar trends to that of n-pentnae except for MO13–MO16 and MO21. From Fig. 6(a) we can see that MO7 shows significant changes both in isopentane and in neopentane but their electron charge density distributions show little change, which is consistent with the cases of the orbital momentum distributions. Also, MO18 presents a similar variation to MO7. However, MO9–MO11 experience larger changes in orbital shape than MO7 and MO18 despite all of them showing significant energy level shifts. As seen in MO9–MO11, partial s electrons all contribute to the orbital construction.

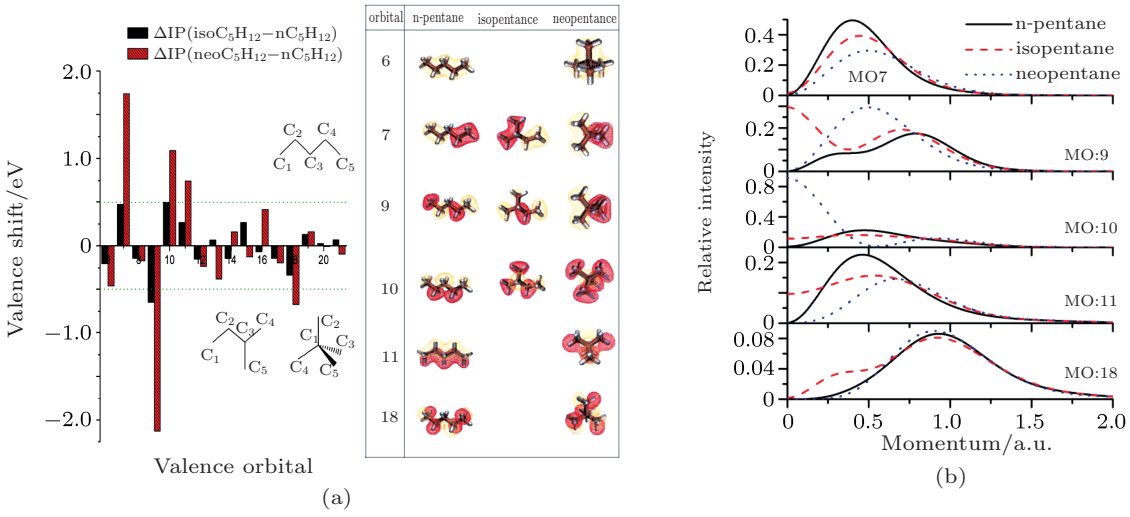


Fig. 6. (colour online) Valence energy shifts (a) and relative intensities (b) of n, iso, neo-C_5H_{12}.

In Figs. 7(a) and 7(b), MO8–MO13 of C_6H_{14} have larger energy level shifts than 0.5 eV and all of them are located in the inner valence space. Of all the six orbitals, MO12 responds the most strongly as its orbital shift is larger than 1.3 eV. Meanwhile, MO11 and MO10 also show more significant variations (with shifts being about 1.0 eV). Similarly, it is easily seen that MO8, MO9, and MO13 also display evident shifts during isomerization. The evident energy level shift could be partially illustrated by the constructed s, p-hybridized orbitals as shown in Fig. 7(b). However, such evident shifts are greatly reduced in the outer valence space particularly in the intermediate valence space as shown in MO20–MO25 and MO14–MO19. Nevertheless, almost all the individual valence orbitals have the same shift trends except for MO15, MO16, MO18, and MO19, which is consistent with the case of pentane. The inconsistent orbital shift can be illustrated by the large dynamic fluctuations in the intermediate valence space. We all know that frontier orbitals are important during chemical reactions. As far as the frontier orbitals are concerned, it is found that the three outermost orbitals have larger IPs than n-hexane, implying that they have the same bonding mechanism and electron rearrangement. Besides, it is clearly seen that the energy level shift shows an ascending order from MO25 to MO23, which can be illustrated by the increased bonding strength. Studies of the orbital momentum distributions of MO8–MO13 give the same conclusions as those from investigations of the energy level shift.

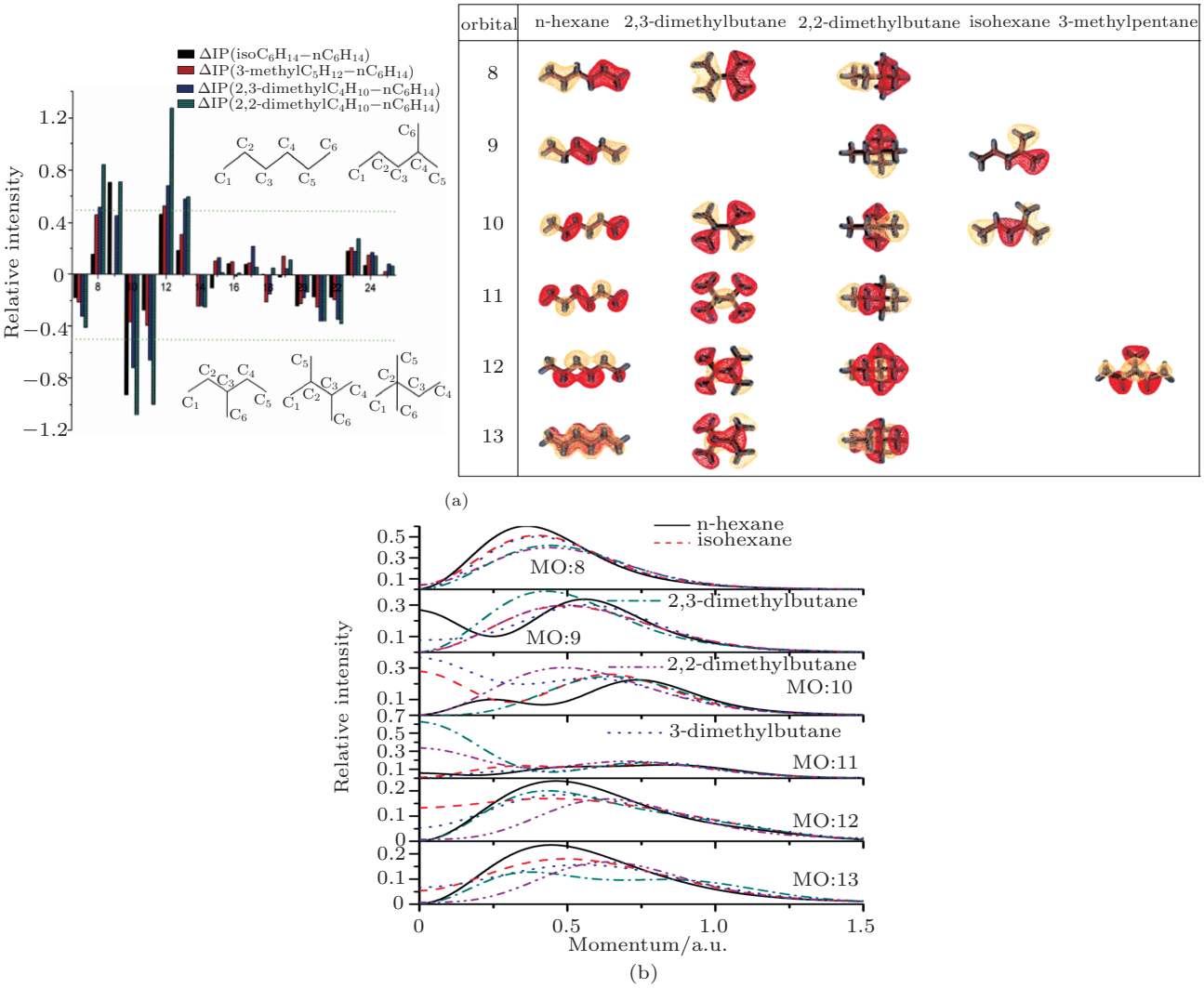


Fig. 7. (colour online) Valence energy shifts (a) and relative intensities (b) of five isomers of C_6H_{14}.

4. Conclusions

Valence orbital responses of C_nH_{2n+2} (n = 1–6) are investigated in momentum and position spaces. The results show that the valence orbitals have strong isomer dependence particularly in lower momentum regions. Investigations on HOMOs show that they are dominated mainly by p-electrons with the exception of isobutane and isopentane which present s, p-hybridized orbitals. Furthermore, we conclude that the relative intensities of the isomers increase with the number of the carbon–carbon bonds in lower momentum regions. The analyses of all the valence orbitals confirm that the exchange effect and the correlation effect play vital roles in the electron redistributions. Further investigations on the representative orbitals demonstrate that the methyl shift can indeed cause electron rearrangement in the whole valence space and thus inevitably introduced different electrons into the orbital construction. An analysis based on the valence energy level shift of C_nH_{2n+2} (n = 4–6) shows that the strong structure dependences of the ionization energy and the opposite energy shift can also be observed in the intermediate valence space.

Acknowledgments

One of the authors, Yang Ze-Jin, thanks the Ministry of Education of China for a Postgraduate Research Scholarship to Australia, and Swinburne University of Technology (SUT, Australia) for its hospitality. He is also grateful to Prof. Wang Feng for supervising his doctoral thesis research at SUT.

References

[1] Hajgato B, Deleuze M S and Morini F 2009 *J. Phys. Chem.* A **113** 7138

[2] Li Z J, Chen X J, Shan X, Liu T and Xu K Z 2009 *J. Chem. Phys.* **130** 054302

[3] Liu K, Ning C G and Deng J K 2009 *Phys. Rev.* A **80** 022716

[4] Luo Z H, Ning C G, Liu K, Huang Y R and Deng J K 2009 *J. Phys.* B: *At. Mol. Opt. Phys.* **42** 165205

[5] Ning C G, Liu K, Luo Z H, Zhang S F and Deng J K 2009 *Chem. Phys. Lett.* **476** 157

[6] Nixon K L, Lawrance W D and Brunger M J 2009 *Chem. Phys. Lett.* **474** 23

[7] Saha S and Wang F 2009 *J. Phys.: Conf. Ser.* **185** 012040

[8] Takahashi M 2009 *Bull. Chem. Soc. Jpn.* **82** 751

[9] Thompson A, Saha S, Wang F, Tsuchimochi T, Nakata A, Imamura Y and Nakai H 2009 *Bull. Chem. Soc. Jpn.* **82** 187

[10] Tu G, Tu Y Q, Vahtras O and Agren H 2009 *Chem. Phys. Lett.* **468** 294

[11] Watanabe N, Chen X J and Takahashi M 2009 *J. Phys.: Conf. Ser.* **194** 052024

[12] Watanabe N and Takahashi M 2009 *J. Phys.: Conf. Ser.* **194** 012018

[13] Yan M, Shan X, Wu F, Xia X X, Wang K D, Xu K Z and Chen X J 2009 *J. Phys. Chem.* A **113** 507

[14] Zhu Q, Wang F and Ivanova E 2009 *J. Synchrotron Rad.* **16** 545

[15] Deleuze M S, Hajgato B, Morini F and Knippenberg S 2010 *J. Phys.: Conf. Ser.* **212** 012020

[16] Liu K, Ning C G and Deng J K 2010 *Chin. Phys. Lett.* **27** 073403

[17] Liu K, Ning C G, Luo Z H, Shi L L and Deng J K 2010 *Chem. Phys. Lett.* **497** 229

[18] Morini F, Hajgato B and Deleuze M S 2010 *J. Phys. Chem.* A **114** 9374

[19] Morini F, Knippenberg S, Deleuze M S and Hajgto B 2010 *J. Phys. Chem.* A **114** 4400

[20] Ren X G, Senftleben A, Pfluger T, Dorn A, Bartschat K and Ullrich J 2010 *J. Phys.* B: *At. Mol. Opt. Phys.* **43** 035202

[21] Shojaei S H R, Hajgato B and Deleuze M S 2010 *Chem. Phys. Lett.* **498** 45

[22] Yang Z J, Guo Y D, Zhu Z H and Yang X D 2010 *Acta Phys. Chim. Sin.* **26** 2523 (in Chinese)

[23] Zhang Z, Kyle O, Hang X M and Chen X J 2010 *Acta Phys. Sin.* **59** 1695 (in Chinese)

[24] Wang K D, Ma P F and Shan X 2011 *Chin. Phys.* B **20** 033102

[25] Cheng Y J and Zhou Y J 2010 *Chin. Phys.* B **19** 063405

[26] Liu J B and Zhou Y J 2010 *Chin. Phys.* B **19** 093403

[27] Hu X Y and Zhou Y J 2010 *Acta Phys. Sin.* **59** 2423 (in Chinese)

[28] Liu K, Ning C G, Shi L L, Miao Y R and Deng J K 2011 *Acta Phys. Sin.* **60** 023402 (in Chinese)

[29] Zhang D L, Tang Q B, Yu B H and Chen D 2011 *Acta Phys. Sin.* **60** 053205 (in Chinese)

[30] Chen Z B, Yang H, Wu X J and Zhang S M 2011 *Acta Phys. Sin.* **60** 063402 (in Chinese)

[31] Gao R J and Ge Z M 2010 *Acta Phys. Sin.* **59** 1702 (in Chinese)

[32] Dey S, Dixon A J, McCarthy I E and Weigold E 1976 *J. Electron Spectrosc. Relat. Phenom.* **9** 397

[33] Weigold E, Dey S, Dixon A J and McCarthy I E 1976 *Chem. Phys. Lett.* **41** 21

[34] Clark S A C, Reddish T J, Brion C E, Davidson E R and Frey R F 1990 *Chem. Phys.* **143** 1

[35] Chen X J, Tian S X, Jia C C, Yu X Q, Yang B Y and Xu K Z 1998 *Acta Phys. Chim. Sin.* **14** 490 (in Chinese)

[36] Fan X W, Zhou S J, Zhang Q X, Deng J K, Zheng Y Y, Gao N F and Chen X J 1998 *Acta Phys. Chim. Sin.* **14** 573 (in Chinese)

[37] Pang W, Shang R, Gao N, Zhang W, Gao J, Deng J, Chen X and Zheng Y 1998 *Phys. Lett.* A **248** 230

[38] Pang W N, Zhang W X, Gao N F, Shang R C, Deng J K and Chen X J 1998 *Chin. Phys. Lett.* **15** 648

[39] Tian S X, Chen X J, Jia C C, Xu C K, Yang B X, Xu K Z, Shuang F and Yang J L 1998 *J. Phys.* B: *At. Mol. Opt. Phys.* **31** 2055

[40] Deng J K, Li G Q, Huang J D, Deng H, Wang X D, Wang F, He Y, Zhang Y A, Ning C G, Gao N F, Wang Y, Chen X J, Zheng Y and Brion C E 1999 *Chem. Phys. Lett.* **313** 134

[41] Jia C C, Chen X J, Tian S X, Oy G, Peng L L, Yang B X, Xu K Z, Yuan L F and Yang J L 1999 *J. Phys.* B: *At. Mol. Opt. Phys.* **32** 1515

[42] Pang W N, Shang R C, Gao N F, Zhang W X, Chen X J, Zheng Y and Brion C E 1999 *Chem. Phys. Lett.* **299** 207

[43] Zheng Y, Pang W N, Shang R C, Chen X J, Brion C E, Ghanty T K and Davidson E R 1999 *J. Chem. Phys.* **111** 9526

[44] Deng J K, Li G Q, He Y, Huang J D, Deng H, Wang X D, Wang F, Zhang Y A, Ning C G, Gao N F, Wang Y, Chen X J and Zheng Y Y 2000 *Chin. Phys. Lett.* **17** 795

[45] Pang W N, Gao J F, Ruan C J, Shang R C, Trofimov A B and Deleuze M S 2000 *J. Chem. Phys.* **112** 8043

[46] Brion C E, Cooper G, Zheng Y, Litvinyuk I V and McCarthy I E 2001 *Chem. Phys.* **270** 13

[47] Deleuze M S, Pang W N, Salam A and Shang R C 2001 *J. Am. Chem. Soc.* **123** 4049

[48] Deng J K, Li G Q, He Y, Huang J D, Deng H, Wang X D, Wang F, Zhang Y A, Ning C G, Gao N F, Wang Y, Chen X J and Zheng Y 2001 *J. Chem. Phys.* **114** 882

[49] Wang F 2003 *J. Phys. Chem.* A **107** 10199

[50] Knippenberg S, Huang Y R, Hajgato B, Francois J P, Deng J K and Deleuze M S 2007 *J. Chem. Phys.* **127** 174306

[51] Wang F and Pang W 2007 *Mol. Simul.* **33** 1173

[52] Schipper P R T, Gritsenko O V, Gisbergen S J A V and Baerends E J 2000 *J. Chem. Phys.* **112** 1344

[53] Velde G T, Bickelhaupt F M, Baerends E J, Guerra C F, Gisbergen S J A V, Snijders J G and Ziegler T *ADF 2008.01 SCM*, Theoretical Chemistry, Vrije University, Amsterdam, the Netherlands

[54] Duffy P, Casida M E, Brion C E and Chong D P 1992 *Chem. Phys.* **165** 183

[55] McCarthy I E and Weigold E 1991 *Rep. Prog. Phys.* **91** 789

[56] Duffy P, Chong D P, Casida M E and Salahub D R 1994 *Phys. Rev.* A **50** 4707

[57] Gritsenko O V, Braida B and Baerends E J 2003 *J. Chem. Phys.* **119** 1937

[58] Gritsenko O V and Baerends E J 2002 *J. Chem. Phys.* **117** 9154

[59] Gritsenko O V, Leeuwen R V and Baerends E J 1994 *J. Chem. Phys.* **101** 8955

[60] Chong D P, Gritsenko O V and Baerends E J 2002 *J. Chem. Phys.* **116** 1760